256/64-QAM Multicarrier Analog Radio-over-Fiber Modulation using a Linear Differential Drive Silicon Mach-Zehnder Modulator

Colm Browning, Alexander Gazman, Nathan Abrams, Keren Bergman, and Liam P. Barry

***Abstract*—Highly linear integrated optical modulators are required in order to provide a distribution platform for analog Radio-over-Fiber (RoF) signals. The work outlined examines the performance of multiple bands of Generalized Frequency Division Multiplexed (GFDM) signals in a photonic link employing a linear differential drive silicon Mach-Zehnder Modulator (MZM). Performance is evaluated in terms of received Bit Error Rate (BER) and Error Vector Magnitude (EVM). In an optical back-to-back scenario, 3.3% EVM is achieved in the case where three GFDM bands modulated with 256 Quadrature Amplitude Modulation (QAM) are transmitted.**

***Index Terms*—Silicon Modulators, 5G, Fronthaul, Photonic Integration.**

I. Introduction

PHOTONIC components and links capable of transmitting analog Radio Frequency (RF) signals hold importance for many applications including beam-steering with phased array antennas [1], satellite communications [2] and millimeter-wave generation [3]. Mobile communications in particular can benefit from the development of enhanced functionality in the optical domain. With 5^{th} Generation (5G) communications on the horizon - for which ultra dense (UD) antenna deployment coupled with Centralized Radio Access Networking (C-RAN) is envisioned [4] - optical distribution of mobile data signals will be key enabling feature.

RoF transmission between Baseband Units (BBUs) and Remote Radio Heads (RRHs), known as fronthaul, is governed by the Common Public Radio Interface (CPRI) recommendation and involves *digital* binary modulation which is easily facilitated due to the maturity of this technology in the optical communication systems. However, as wireless networks scale and move toward UD antenna distribution, the transmission of *analog* RoF formats offers the advantage of decreased complexity at the RRH through the avoidance of Digital-to-Analog Converters (DAC) at each antenna site. For such links; due to the analog nature of the driving signal, a highly linear mapping to the optical domain is required in order to avoid signal distortion. Commercially available optical modulators are typically designed for Non-Return to Zero (NRZ) modulation with a limited range of linear operation.

Silicon Photonics (SiP) has emerged as the leading technology for the development of Photonic Integrated Circuits (PICs). This is due to its ability to provide a wide range of optical functionality in a small footprint and cost effective PIC which is compatible with Complementary Metal Oxide Semiconductor (CMOS) processes. Indeed, SiP modulators based on MZ interferometer [5], Micro Ring Resonator (MRR) [6] and Electro Absorption (EA)[1] structures have all previously been demonstrated. As the optical world embraces SiP technology, it is important to assess to what degree these new integrated component designs are compatible with emerging RoF technologies - for which optical modulation and distribution are among the key facilitating factors.

Multi-carrier analog modulation using silicon based optical modulators has previously been demonstrated in [7] and [8]. [7] makes use of single ended silicon MZM to transmit broadband Orthogonal Frequency Division Multiplexing (OFDM) where each subcarrier is modulated with 16-QAM. The single drive push-pull silicon MZM demonstrated in [8] is used to modulate a broadband Discrete Multi-Tone (DMT) signal which exhibits differing modulation levels across its subcarriers - maximizing at 128-QAM.

In this work we makes use of a traveling-wave silicon MZM (Si-MZM) based on the carrier depletion effect which exhibits improved linearity through the device's differential drive implementation [9]. The Si-MZM is used to optically modulate up to 10 bands of 'narrow-band' 64/256-QAM 5G candidate waveform GFDM [10]. Compared to 4G waveform OFDM, GFDM's Inverse Fast Fourier transform (IFFT) based implementation exhibits the same subcarrier spacing but employs circular filtering which minimizes overlapping between subcarriers - increasing GFDM's tolerance to timing synchronization errors [10]. Results show the successful back-to-back transmission of up to 10 bands of 64-QAM GFDM, and 3 bands of 256-QAM GFDM highlighting the Si-MZM's suitability for next generation integrated mobile fronthaul.

II. Linear Differential Drive Si-MZM

The basic structure of the Si-MZM is shown as part of the setup in 1. The device consists of two parallel depletion mode PN junction phase shifters used for RF modulation. Both

C. Browning and L.P. Barry are with the School of Electronic Engineering, Dublin City University, Dublin D09W6Y4, Ireland. e-mail: colm.browning@dcu.ie

A. Gazman, N. Abrams and K. Bergman are with the Department of Electrical Engineering, Columbia University, New York 10027, United States.

This collaboration was supported by the Higher Education Authority (HEA) of Ireland Mobility programme. The publication has also emanated from research supported in part by a research grant from Science Foundation Ireland (SFI) under grant numbers 13/RC/207 (CONNECT), and jointly with the National Science Foundation (NSF) 15/US-C2C/I3132 (US-Ireland Partnership). The work was also supported through FA8650 (AIM Photonics) and EEC-0812072 (CIAN NSF ERC).

978-1-5386-5226-8/18/$31.00 ©2018 IEEE

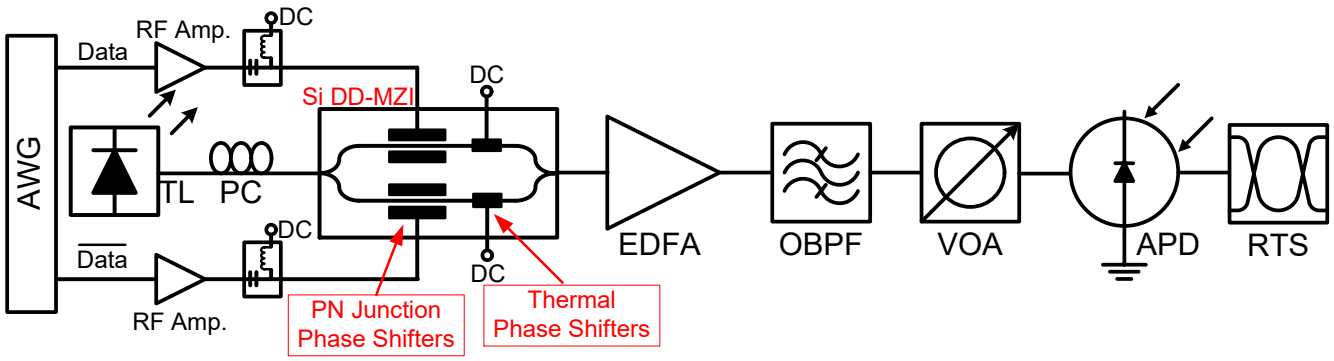

Fig. 1: Optical back-to-back RoF setup including Si-MZM structure outline.

arms have an associated thermal phase shifter which allows optimum biasing of the unbalanced device at all wavelengths. Further details of the device fabrication can be found in [12].

This silicon device structure has previously been characterized in [9] which finds that under two tone testing conditions, the third order Inter-modulation Distortion Spur Free Dynamic Range (SFDR_{IMD}) is 92 dB·$\text{Hz}^{\frac{2}{3}}$ when a single arm of the modulator is used. By differentially driving the modulator SFDR_{IMD} increases to 97 dB·$\text{Hz}^{\frac{2}{3}}$. The V_π of the modulator is ∼5V. Light is coupled to and from the chip via grating couplers and the total loss (including those due to packaging) is about 15 dB. The modulation bandwidth of the device alone is measured to be 15 GHz although packaging resulted additional frequency roll-off.

III. Experimental Setup

TABLE I: GFDM signal properties.

Property	64-QAM	256-QAM
Bandwidth	150 MHz	150 MHz
FFT size	1024	1024
Cyclic prefix	6.25%	6.25%
No. Subcarriers	154	154
Nbr. Bands	10	3
Data Rate per band	0.9 Gb/s	1.2 Gb/s

The experimental setup is shown in Fig. 1. GFDM bands (or channels) are generated in Matlab with the properties outlined in Tab. I. Provided fiber non-linearities are avoided, negligible impact due to propagation is expected as dispersion can be overcome through the inclusion of a Cyclic Prefix (CP). The GFDM bands are digitally mixed to intermediate frequencies around 1.5 GHz such that a 15 MHz guard-band exists between each band. The composite signal was loaded into a Keysight Arbitrary Waveform Generator (AWG) which operated at 60 GSa/s. Complementary outputs of the AWG were amplified to $\sim 4.5\text{V}_{\text{pk-pk}}$ and used to differentially drive the Si-MZM after DC bias voltages are added via bias tees. Light from a Tunable Laser (TL) set to operate at 1545 nm with an output power of 10 dBm is coupled to the modulator via a Polarization Controller (PC). The output of the modulator is then amplified using an Erbium Doped Fiber Amplifier (EDFA) which is used to overcome packaging losses and

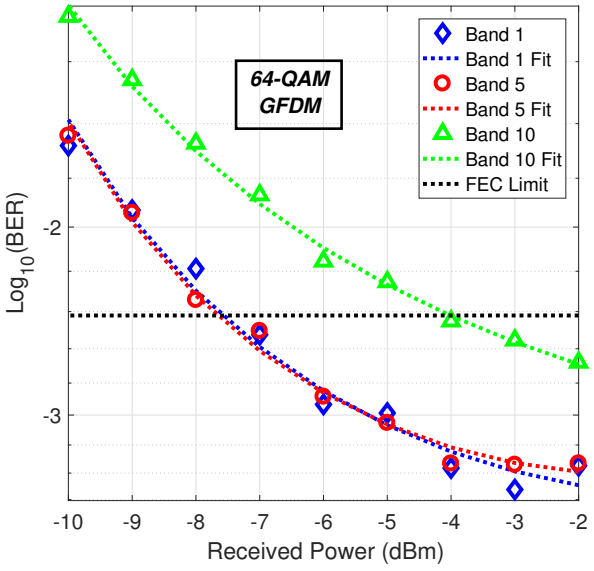

Fig. 2: Received power versus BER for bands 1, 5 and 10 of the 10 band 64-QAM GFDM modulated signals.

provide dynamic range for BER measurement. An Optical Bandpass Filter (OBPF) suppresses Amplified Spontaneous Emission (ASE) before a Variable Optical Attenuator (VOA) sets the optical power falling on the Avalanche Photo-diode (APD) based receiver. The electrical signal is sampled by a Tektronix Real Time Oscilloscope (RTS) at 50 GSa/s. Channel estimation, equalization, demodulation as well as BER and EVM calculations are performed offline in Matlab.

IV. Result and Discussion

Fig. 2 shows received optical power versus BER for bands 1, 5 and 10 of the 10 band 64-QAM composite GFDM transmitted signal. These bands have corresponding center frequencies of 0.65, 1.33 and 2.17 GHz respectively. In all cases performances below the 7% Forward Error Correction (FEC) limit (3.8×10^{-3}) is achieved. Bands 1 and 5 exhibit similar performances, reaching 3×10^{-4} for a received power of -3 dBm in the case of band 1.

At the FEC limit a 4 dB penalty between band 1 and band 10 can be observed. This can be explained by examining the

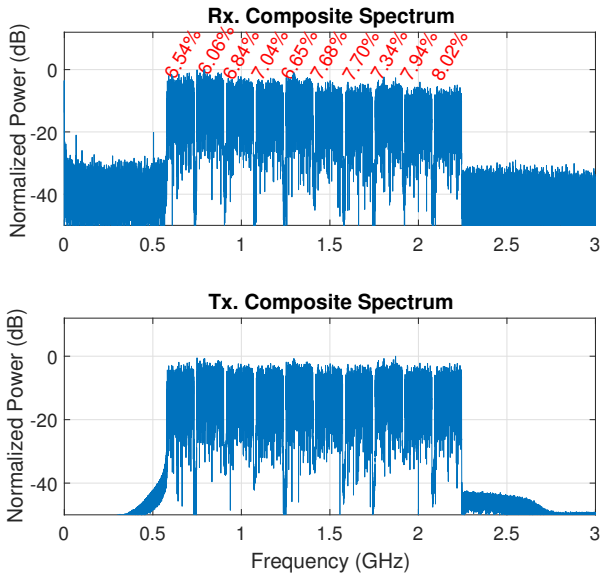

Fig. 3: Received (Rx.) and transmitted (Tx.) RF spectra of the composite 10 band 64-QAM GFDM signals.

spectral response evident in Fig. 3 which shows the received RF spectrum of the composite GFDM signal (above) and the transmitted spectrum for reference (below). A power spectral roll-off of ∼4 dB can be observed between band 1 and band 10 and this is due to the packaging of Si-MZM. Fig. 3 also shows EVM achieved on each GFDM band for a received power of -3 dBm. As well as the frequency roll-off, differing Peak-to-Average Power Ratios (PAPR) also lead to slight variations in the performances of each band. The PAPR of the composite signal, of 14.8 dB, was reduced to 12 dB by hard clipping. In all cases performances below the FEC threshold were achieved.

Fig. 4 shows the performance in terms of BER for all bands

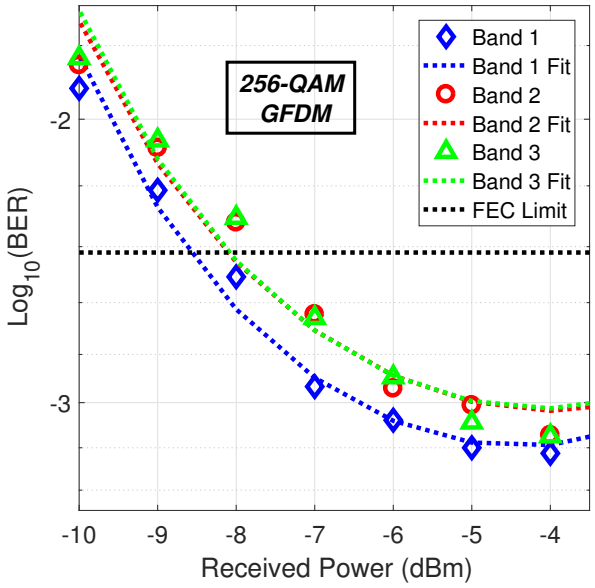

Fig. 4: Received power versus BER for three bands of 256-QAM GFDM.

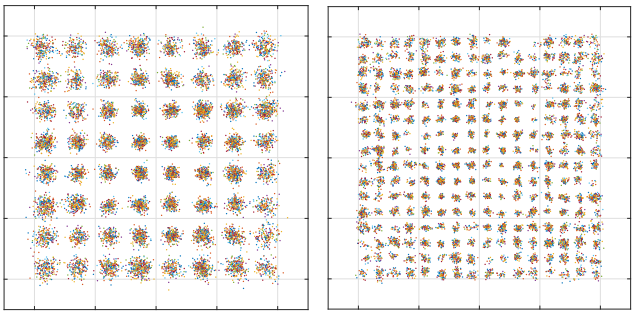

(a) Band 1, 64-QAM, -3dBm. (b) Band 3, 256-QAM, -4dBm.

Fig. 5: Received GFDM constellations for all respective 64 and 256-QAM modulated subcarriers.

(1, 2 and 3) of the 256-QAM GFDM signal, as the power falling on the PD is varied. The center frequencies of the bands are 1.83, 2 and 2.17 GHz respectively. The figure shows that when 256-QAM (8 amplitude levels) is used, BERs achieved (down to 5.9×10^{-4} for band 1 at -4 dBm) are similar to those exhibited in the 64-QAM cases (6 amplitude levels) - indicating improved performance in this regime. This is more apparent when EVMs are compared. Under optimum conditions, the 256-QAM GFDM bands 1, 2 and 3 result in received EVMs of 3.3%, 3.54% and 3.58% respectively, while the equivalent (in center frequency) 64-QAM bands (8, 9 and 10) give 7.34%, 7.94% and 8.02%.

There are two reasons for this disparity in performance, both of which stem from the fact that a different number of bands are transmitted in each case. Firstly, although the Si-MZM exhibits high linearity, some non-linearity is present resulting in the inter-mixing of GFDM subcarriers, the products of which may fall in-band. This effect is exacerbated when 1000's of subcarriers are transmitted in tandem to effectively form a broadband multi-carrier spectrum, as is the case when 10 bands of GFDM are modulated. Secondly, increasing the total number of transmitted subcarriers statistically leads to higher PAPR due to the increased potential for peaking due subcarrier addition. Indeed, in the experiment described, the 3 band 256-QAM GFDM case resulted in a PAPR of 12.3 dB which, after hard clipping, was reduced to 10.3 dB; 1.7 dB lower than the 10 band case. A lower PAPR in the context of an analog driving signal leads to more efficient use of the modulators linear region, and ultimately enhanced performance.

Fig. 5(a) and (b) show example 64 and 256-QAM constellations, respectively, of all subcarriers associated with a single band received under optimum conditions. From Fig. 5(a) some non-linearity arising from the Si-MZM transfer characteristic is apparent as higher amplitude constellation points are more distorted compared to lower amplitude ones.

V. Conclusion

Increased centralization and UD deployment associated with future mobile networks will lead to greater convergence between the radio and optical communications systems. SiP technology will allow the development of cost effective, and flexible optical PICs, but in order to facilitate the functionalities envisioned for next generation wireless networks, must be

capable of handling analog RF modulation and distribution. Silicon modulators are a key building block of such PICs, and the work presented in this paper shows the successful modulation of multiple 256/64-QAM GFDM '5G' bands using a linear differential drive silicon MZM. Performance as low as 3.3% EVM is achieved highlighting the ability of the Si-MZM to provide effective analog RoF modulation. Furthermore, the results indicate SiP's potential to facilitate integrated optical-wireless networking.

REFERENCES

[1] C. T. Phare, J. Cardenas, Y. H. D. Lee and M. Lipson, "Linear graphene on silicon nitride electroabsorption modulators for RF-over-fiber links," CLEO, San Jose, CA, 2016.

[2] K. Xu, *et al.*, "Microwave photonics: radio-over-fiber links, systems, and applications [Invited]," Photon. Res. 2, B54-B63, 2014.

[3] C. Browning, E. P. Martin, A. Farhang and L. P. Barry, "60 GHz 5G Radio-Over-Fiber Using UF-OFDM With Optical Heterodyning," in IEEE PTL, vol. 29, no. 23, pp. 2059-2062, 2017.

[4] J. G. Andrews et al., "What Will 5G Be?" in IEEE J. on Sel. Commun., vol. 32, no. 6, p. 1065, 2014.

[5] A. M. Gutierrez *et al.*, "High linear ring-assisted MZI electro-optic silicon modulators suitable for radio-over-fiber applications," GFP, San Diego, CA, 2012.

[6] Q. Xu, B. Schmidt, J. Shakya, and M. Lipson, "Cascaded silicon micro-ring modulators for WDM optical interconnection,"" Opt. Express Vol. 14, pp. 9431-9436, 2006.

[7] K. Xu, *et al.*, "Experimental Demonstration of Multi-level Modulation on OFDM Signals Using Integrated Silicon Modulators," in OFC paper OW1G.5, 2013.

[8] P. Dong, *et al.*, "Four-Channel 100-Gb/s per Channel Discrete Multi-Tone Modulation Using Silicon Photonic Integrated Circuits," in OFC Post Deadline, paper Th5B.4, 2015.

[9] M. Streshinsky *et al.*, "Highly linear silicon traveling wave Mach-Zehnder carrier depletion modulator based on differential drive," Opt. Express, Vol. 21, pp. 3818-3825, 2013.

[10] B. Farhang-Boroujeny and H. Moradi, "OFDM Inspired Waveforms for 5G," in IEEE Commun. Surv. Tutor., vol. 18, no. 4, pp. 2474-2492, 2016.

[11] A. Aminjavaheri, A. Farhang, A. Rezazadeh-Reyhani and B. Farhang-Boroujeny, "Impact of timing and frequency offsets on multicarrier waveform candidates for 5G," SP/SPE, Salt Lake City, UT, pp. 178-183, 2015.

[12] M. Streshinsky *et al.*, "Silicon Parallel Single Mode 48 50 Gb/s Modulator and Photodetector Array," in J. Lightwav. Technol., vol. 32, no. 22, pp. 4370-4377, 2014.